JCTC Journal of Chemical Theory and Computation

Article

pubs.acs.org/JCTC

Benchmark Many-Body *GW* and Bethe–Salpeter Calculations for Small Transition Metal Molecules

Sabine Körbel,[†] Paul Boulanger,[‡,§] Ivan Duchemin,[∥] Xavier Blase,[‡,§] Miguel A. L. Marques,[†] and Silvana Botti*[,†]

[†]Institut Lumière Matière and European Theoretical Spectroscopy Facility, UMR5306 Université Lyon 1-CNRS, Université de Lyon, F-69622 Villeurbanne Cedex, France

[‡]Univ. Grenoble Alpes, Inst NEEL, F-38042 Grenoble, France

[§]CNRS, Inst NEEL, F-38042 Grenoble, France

[∥]INAC, SP2M/L_sim, CEA cedex 09, 38054 Grenoble, France

Supporting Information

ABSTRACT: We study the electronic and optical properties of 39 small molecules containing transition metal atoms and 7 others related to quantum-dots for photovoltaics. We explore in particular the merits of the many-body *GW* formalism, as compared to the ΔSCF approach within density functional theory, in the description of the ionization energy and electronic affinity. Mean average errors of 0.2–0.3 eV with respect to experiment are found when using the PBE0 functional for ΔSCF and as a starting point for *GW*. The effect of partial self-consistency at the *GW* level is explored. Further, for optical excitations, the Bethe–Salpeter formalism is found to offer similar accuracy as time-dependent DFT-based methods with the hybrid PBE0 functional, with mean average discrepancies of about 0.3 and 0.2 eV, respectively, as compared to available experimental data. Our calculations validate the accuracy of the parameter-free *GW* and Bethe–Salpeter formalisms for this class of systems, opening the way to the study of large clusters containing transition metal atoms of interest for photovoltaic applications.

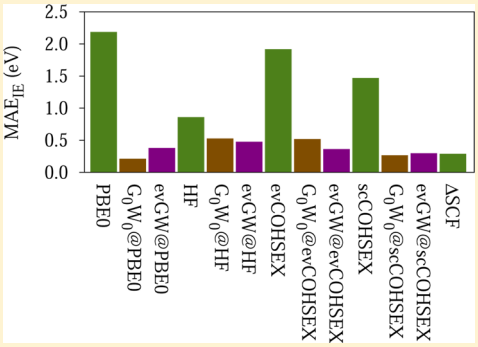

1. INTRODUCTION

Electronic ground- and excited state properties of molecules can be modeled very accurately using many-body wave function quantum-chemistry methods. However, such calculations are computationally expensive and scale unfavorably with the size of the system and are therefore mainly feasible for small molecules.[1−3] For larger molecules and nanoparticles, suitable theoretical approximations are needed to lower the computational burden, while assuring a satisfying level of accuracy. Theories such as Hartree–Fock (HF) and, even more, density functional theory (DFT), are appealing as they are computationally efficient. Within DFT, (semi)local approximations to the exchange-correlation functional, such as the local-density approximation (LDA)[4] or the generalized-gradient approximation (GGA),[5] can yield reasonably good ground-state total energies.[3] DFT-LDA one-particle energy eigenvalues can qualitatively agree with experiment; however, the energy gaps are severely underestimated,[3] whereas in Hartree–Fock theory they are usually strongly overestimated.[2] Band gaps of semiconductors obtained with hybrid functionals (such as B3LYP,[6] PBE0,[7] HSE[8]), which contain a fraction of Hartree–Fock exchange, were found to be in much better agreement with experiment than those from (semi)local functionals.[9−11] For a series of 34 molecules, however, using the PBE0 functional, Rostgaard et al.[12] obtained HOMO energies which deviate by 2.55 eV on average from experimental ionization energies. The authors conclude that the amount of HF exchange needed to reproduce experiment is highly system-dependent.

A much more accurate way to access one-particle excitations in finite systems based on DFT and its hybrid generalization are ΔSCF calculations.[2] The ΔSCF method has also been extended and applied to higher excited states, but becomes impracticable for large systems with many low-lying states,[13] and its accuracy depends on the ability of the exchange-correlation functional in DFT to yield correct ground-state energies, which is not always the case.

In a solid, where it is not obvious to carry out ΔSCF calculations, since there is no localized state whose occupation can be varied, many-body Green's function-based approaches have been found to be extremely successful to predict the ionization energies and the band gaps of materials.[2,3] The *GW* approximation to the self-energy is usually used in Hedin's equations.[14] Hedin's equations should in principle be solved self-consistently, which can easily make the computational burden very large. Therefore, the *GW* correction to a prior self-consistent calculation within a simpler approximation is very

Received: April 25, 2014
Published: July 23, 2014

   dx.doi.org/10.1021/ct5003658 | J. Chem. Theory Comput. 2014, 10, 3934–3943

often evaluated perturbatively (G_0W_0). The final result thus depends on the choice of the approach chosen as a starting point.[2,15] Another way to make calculations more efficient consists in neglecting the frequency dependence of the screening of the Coulomb potential in W, such as in the Coulomb-hole plus screened exchange (COHSEX) approximation to the GW self-energy.[14]

GW approaches have been much less used for atoms and molecules than for solids, but several authors have recently performed comparative GW calculations for molecules in the gas phase.[12,15−27] Blase et al.[17] applied different levels of GW to a set of molecules relevant for organic photovoltaics, including C_{60}. The authors compared ionization energies and quasiparticle gaps from G_0W_0 and self-consistent GW (where the self-consistency is restricted to the eigenvalues) starting from LDA or Hartree−Fock-like eigenvalues. They found a similar agreement with experiment for self-consistent GW and perturbative G_0W_0 starting from Hartree−Fock eigenvalues. Similarly, excellent agreement with high-level many-body quantum chemistry techniques (CASPT2, EOM-IP-CCSD) was obtained for the frontier orbitals of DNA and RNA nucleobasis.[28]

Rostgaard et al.[12] performed fully self-consistent PAW-GW calculations for a large set of small molecules and systematically investigated the effects of core−valence interactions and self-consistency.

Bruneval and Marques[15] compared different DFT functionals as starting points for G_0W_0 calculations. The authors concluded that hybrid functionals, especially those with a large HF-exchange contribution, are the best starting point for a GW calculation.

In this work, we apply different approximations to GW, using both self-consistent and perturbative GW on top of several starting points (DFT-PBE0, Hartree−Fock, self-consistent (sc) COHSEX), to a set of small transition metal molecules and a few others related to thin-film photovoltaics, in order to systematically evaluate their agreement with experimental data and ΔSCF calculations. We also aim to identify by means of benchmark calculations which GW scheme represents the best compromise between computational cost and accuracy, in order to prepare a further study of larger nanostructures containing transition metals, which are promising for applications as absorbers in the new generation of thin-film solar cells. Although $Cu(InGa)Se_2$ (CIGS) is one of the most widely used thin-film absorber material, indium-free alternatives, such as $Cu_2ZnSn(S,Se)_4$ (CZTS), have already begun to replace CIGS, in order to reduce the material costs. Thin films of CZTS can be made by depositing a solvent containing CZTS nanoparticles on a substrate. The required homogeneous film is obtained by sintering. Another possible application for CZTS are quantum-dot sensitized solar cells. In both cases, the dependence of the optical absorption gap on the grain size or quantum-dot size is of interest. Whereas the optical properties of clusters made of Si have been investigated,[29,30] only little is known about the size-dependence of the optical gap for CZTS clusters. An experimental study[31] reported an optical gap opening at a cluster diameter between 2 and 5 nm. A few ab initio calculations of optical spectra of bulk CIGS and CZTS(e) have already been published by other groups.[32,33] For bulk CZTS and other transition metal compounds, a single-shot GW calculation (G_0W_0) after a self-consistent COHSEX run has been shown to be very successful.[34] Here, we will determine whether the same approach is suitable for (small) molecules of the same elements as well.

In order to model neutral electronic excitations, such as light absorption, in molecules, accurate one-particle energy levels are not always sufficient because the electron−hole interaction may become important. The Bethe−Salpeter equation (BSE), which includes the latter, has been successfully applied for modeling optical excitations both of extended solids and of atoms and molecules.[2] Even though less documented than for bulk systems, the merits of the BSE approach for gas phase molecules has recently gained increasing attention.[24,26,35−44] Time-dependent density-functional theory (TDDFT) is, in principle, equally suitable and computationally less expensive, but its accuracy depends strongly on the underlying exchange-correlation functional, and is size and system dependent. Whereas TDDFT within the local-density approximation (TDLDA) has been successfully applied to small systems, it does not reproduce the experimental spectrum of, for example, bulk silicon.[2] Here, we compare results obtained with both the BSE and TDDFT, using a hybrid functional, for our set of small molecules, but we stress that the TDDFT approach may not be successful for larger cluster sizes.

This paper is organized as follows. In section 2, we describe the computational details of our ab initio calculations. In section 3, we estimate the possible errors caused by the incompleteness of the Gaussian basis, the pseudopotential approach, and the use of an auxiliary basis. We then compare ionization energies, electron affinities, and optical gaps, obtained at different levels of theory, with available experimental data. We discuss all results in section 4, and close with a summary.

2. METHODS AND COMPUTATIONAL DETAILS

2.1. DFT Geometry Optimization. Our calculations are performed at the computed equilibrium geometry, obtained by minimizing the total energy of the molecules within DFT using the code NWChem,[45] with the hybrid PBE0 exchange-correlation functional,[7] a Gaussian basis, and atomic pseudopotentials (except for H). The choice of using pseudopotentials is motivated by our intention to run GW calculations for larger clusters in the future. We tested very carefully the quality of the pseudopotentials against all-electron calculations. Note that pseudopotentials of transition metals include semicore electrons in the valence. It is known that special care must be taken in the core−valence partition for GW calculations.[46] In principle, the self-energy should contain an appropriate core−valence exchange interaction, which is only modeled at the LDA level, if the semicore states are included in the core. For this reason, GW corrections can carry a substantial error when the spatial overlap between the valence and the semicore wave functions is sizable.[47,48] On the other hand, it was found that, when semicore states are included in the valence, GW corrections are reliable.[49,50]

According to Bruneval and Marques,[15] a quadruple-ζ basis plus polarization is needed to converge the ionization energies of isolated atoms and small molecules within 0.1 eV, while for a double-ζ basis plus polarization, the basis set error of the HOMO energy is about 0.5 eV. We have thus chosen to augment the "sbkjc-vdz-ecp" double-ζ Gaussian basis set of refs 51, 52, and 53, associated with the corresponding "sbkjc-ecp" pseudopotentials, with the polarization and augmentation functions of the correlation-consistent quadruple-ζ plus polarization ("aug-cc-pvqz") set of refs 54, 55, and 56. In this way,

dx.doi.org/10.1021/ct5003658 | J. Chem. Theory Comput. 2014, 10, 3934−3943

we take advantage of the smooth semicore and valence wave functions of the "sbkjc-vdz-ecp" basis while maintaining the accuracy of the "aug-cc-pvqz" basis. Our basis, in the following named "aug-sbkjc-pp", includes semicore states of the transition metals in the valence. Geometries obtained with the "aug-sbkjc-pp" basis are in good agreement with experiment (see below and Supporting Information), and ionization energies and electron affinities are well converged compared to the all-electron "aug-cc-pvqz" basis (see Supporting Information).

The geometries are optimized until energy differences of consequent steps fall below 10^{-6} Hartree, and the maximum force below 1.8×10^{-3} Hartree/Bohr.

2.2. Quasiparticle Energies and Energy Gaps. In the *GW* approximation, the self-energy Σ, which replaces the exchange-correlation potential, reads

$$\Sigma(\mathbf{r}, \mathbf{r}', \omega) = \frac{\mathrm{i}}{2\pi} \int \mathrm{d}\omega' \mathrm{e}^{\mathrm{i}0^+\omega'} G(\mathbf{r}, \mathbf{r}', \omega + \omega') W(\mathbf{r}, \mathbf{r}', \omega') \tag{1}$$

where W is the screened Coulomb interaction and G is the time-ordered one-particle Green's function:

$$G(\mathbf{r}, \mathbf{r}', \omega) = \sum_n \frac{\phi_n(\mathbf{r})\phi_n^*(\mathbf{r}')}{\omega - \varepsilon_n + \mathrm{i}0^+ \mathrm{sign}(\varepsilon_n - \mu)} \tag{2}$$

with μ equal to the electronic chemical potential. The energies ε_n in eq 2 are electron addition and removal energies, which can be fixed to a value determined by the starting point of a perturbative G_0W_0 calculation, or can be updated in self-consistent *GW* cycles until a converged value is reached. In the following *GW* calculations, only the quasiparticle energies are updated, while the ϕ_n orbitals are kept fixed. We label this efficient partial self-consistent approach "ev*GW*".

The screened Coulomb interaction W is obtained from the Dyson equation:

$$W(\mathbf{r}, \mathbf{r}', \omega) = v(\mathbf{r}, \mathbf{r}') + \int \mathrm{d}\mathbf{r}'' \int \mathrm{d}\mathbf{r}''' v(\mathbf{r}, \mathbf{r}'') \chi^0(\mathbf{r}'', \mathbf{r}''', \omega) \times W(\mathbf{r}''', \mathbf{r}', \omega) \tag{3}$$

where χ^0 is the independent-particle susceptibility,

$$\chi^0(\mathbf{r}, \mathbf{r}', \omega) = -\frac{\mathrm{i}}{\pi} \int \mathrm{d}\omega' G(\mathbf{r}, \mathbf{r}', \omega + \omega') G(\mathbf{r}', \mathbf{r}, \omega') \tag{4}$$

and v is the Coulomb interaction. The quasiparticle energy of the state n, $\varepsilon_n^{\mathrm{QP}}$, is evaluated as a first-order perturbation of the Kohn–Sham energy level, $\varepsilon_n^{\mathrm{KS}}$,

$$\varepsilon_n^{\mathrm{QP}} = \varepsilon_n^{\mathrm{KS}} + \langle n | \Sigma^{GW}(\varepsilon_n^{\mathrm{QP}}) - V_{xc} | n \rangle \tag{5}$$

where V_{xc} is the exchange-correlation potential in DFT. A more detailed description of this *GW* implementation has been given in ref 17.

In the static COHSEX approximation, only $W(\omega = 0)$ is taken into account, leading to

$$\Sigma^{\mathrm{COHSEX}} = -\sum_n \phi_n(\mathbf{r})\phi_n^*(\mathbf{r}')\Theta(\mu - \varepsilon_n) W(\mathbf{r}', \mathbf{r}, \omega = 0) + \frac{1}{2}(W(\mathbf{r}', \mathbf{r}, \omega = 0) - v(\mathbf{r}, \mathbf{r}'))\delta(\mathbf{r} - \mathbf{r}') \tag{6}$$

where Θ is Heaviside's step function. Due to the reduced cost of this static *GW* approximation, full self-consistency on both eigenvalues and eigenstates can be performed, a scheme that we label "scCOHSEX".

We use the code Fiesta,[17,42] which is based on a Gaussian-basis implementation of the *GW* formalism. The energy integration in eq 1 is performed along the imaginary axis thanks to contour-deformation techniques. The one-body wave functions ϕ_n are expanded at the "aug-sbkjc-pp" basis level (see above). Two-point functions $f(\mathbf{r},\mathbf{r}')$ are expanded in an auxiliary Gaussian basis[17,57,58] $\mu(\mathbf{r})$ using the resolution of the identity with a Coulomb metric (RI-V),[59] such that four-center Coulomb integrals $\langle jk|v|lm\rangle$ between basis functions j, k, l, and m read

$$\langle jk|v|lm\rangle = \sum_{\mu\lambda} \langle jk|v|\mu\rangle V^{-1}_{\mu\lambda} \langle \lambda|v|lm\rangle \tag{7}$$

with

$$\langle jk|v|\mu\rangle = \int \mathrm{d}\mathbf{r} \int \mathrm{d}\mathbf{r}' j(\mathbf{r}) k(\mathbf{r}) v(\mathbf{r}, \mathbf{r}') \mu(\mathbf{r}') \tag{8}$$

and

$$V_{\mu\lambda} = \int \mathrm{d}\mathbf{r} \int \mathrm{d}\mathbf{r}' \mu(\mathbf{r}) v(\mathbf{r}, \mathbf{r}') \lambda(\mathbf{r}') \tag{9}$$

The auxiliary basis functions are of the form

$$\mu(\mathbf{r}) = c\, \mathrm{e}^{-\alpha r^2} r^l R_{lm}(\theta, \phi) \tag{10}$$

where the R_{lm} are real spherical harmonics. As in ref 17, we use an even-tempered auxilary basis (α_i/α_{i+1} = constant). The auxiliary basis is defined by the maximum and minimum radial decay coefficient α, and the number of different coefficients for each angular momentum number. Since the auxiliary basis represents products of basis functions, we choose as minimum and maximum coefficients those which correspond to twice the minimum and maximum ones of the DFT basis. We find that four to eight radial functions per atom and angular channel are sufficient for our systems. Angular momentum numbers up to l = 4 are included in the auxiliary basis. The auxiliary basis has been validated by increasing the number of Gaussians per l-channel, and also by comparing the results of Hartree–Fock calculations performed with NWChem without any auxiliary basis and Hartree–Fock calculations performed with Fiesta with the auxiliary basis (see Supporting Information). All occupied and virtual states are included in the calculation of the time ordered Green's function and the independent particle susceptibility.

Both perturbative G_0W_0 and ev*GW* calculations are performed, either starting from DFT-PBE0 Kohn–Sham orbitals, Hartree–Fock, or scCOHSEX quasiparticle states. Further, following the simple ev*GW* scheme, we also test as a starting point a partially self-consistent COHSEX scheme where only the eigenvalues are updated, keeping the input PBE0 wave functions frozen. We label this evCOHSEX. In the following, we use the notation "*GW* approach@starting point"; for example, ev*GW*@PBE0 indicates a (partially) self-consistent *GW* calculation starting from PBE0 eigenstates. The different levels of theory and self-consistency are listed in Table 1.

In the perturbative G_0W_0 and the ev*GW* steps, we perform the *GW* corrections for three to ten occupied and unoccupied states each. States that are not corrected are rigidly shifted, preserving the energy spacing of the input eigenstates. The energy levels of the ev*GW* calculations are typically converged within a few millielectron volts (meV) or less in five to seven iterations.

In order to estimate atomic relaxation effects, we also perform vertical and adiabatic ΔSCF calculations using the

Table 1. Different Levels of Theory and Selfconsistency on Wavefunctions (WF) and Eigenvalues (EV) Used Here

	self-consistency on	
theory	WF	EV
evCOHSEX	–	×
scCOHSEX	×	×
G_0W_0	–	–
evGW	–	×

PBE0 functional. The ionization energies (IE) and electron affinities (EA) in ΔSCF are defined as

$$\mathrm{IE}(\Delta\mathrm{SCF}) = E_{\mathrm{tot}}^{+1} - E_{\mathrm{tot}}^{\mathrm{neutral}}$$
$$\mathrm{EA}(\Delta\mathrm{SCF}) = E_{\mathrm{tot}}^{\mathrm{neutral}} - E_{\mathrm{tot}}^{-1} \quad (11)$$

where $E_{\mathrm{tot}}^{\mathrm{neutral}}$, E_{tot}^{+1}, and E_{tot}^{-1} are the total energies of the neutral molecules and the molecules with a missing and an additional electron, respectively.

Experimental numbers used for comparison, taken from refs 60, 61, and 62−103, are averaged. The spread of the experimental data is given in the Supporting Information.

2.3. Optical Gaps. Optical gaps are obtained by solving the Bethe−Salpeter equation (BSE) on top of evGW@PBE0 states using the code Fiesta, and from time-dependent density-functional theory (TDDFT) with the PBE0 functional (TDPBE0) using the code NWChem. The BSE reads

$$L = (1 - L_0\Xi)^{-1}L_0 \quad (12)$$

where L is the interacting-particle polarizability, and $\Xi = i\delta\Sigma/\delta G \approx v - W$ is the BSE kernel. The BSE can be rewritten in the electron−hole basis,[104] $\Phi n_1 n_2(\mathbf{r}_1, \mathbf{r}_2) = \phi_{n_1}(\mathbf{r}_1)\phi^*_{n_2}(\mathbf{r}_2)$, as

$$L_{n_1n_2n_3n_4}(\omega) = (\mathcal{H}^{exc} - \omega)^{-1}_{n_1n_2n_3n_4}(f_{n_1} - f_{n_2}) \quad (13)$$

where the excitonic Hamiltonian reads

$$\mathcal{H}^{exc}_{n_1n_2n_3n_4} = (\varepsilon^{\mathrm{QP}}_{n_2} - \varepsilon^{\mathrm{QP}}_{n_1})\delta_{n_1n_3}\delta_{n_2n_4} + (f_{n_1} - f_{n_2})\Xi_{n_1n_2n_3n_4} \quad (14)$$

Here, the $\varepsilon^{\mathrm{QP}}_n$ and f_n are the energies and occupation numbers of quasiparticle states ϕ_n, respectively. The two-point susceptibility, relevant for light absorption, is obtained from the four-point function $L(1,2;3,4)$ as $\chi(1,2) = L(1,2;1,2)$. In TDDFT, the equation to solve for χ reads

$$\chi = (1 - \chi_0\mathcal{K})^{-1}\chi_0 \quad (15)$$

where χ_0 is the independent-particle susceptibility, and $\mathcal{K} = v + \delta V_{xc}/\delta n$, n being the electronic density, is the TDDFT kernel. Equations 13 and 15 are solved by a Davidson diagonalization. Coupling terms between resonant and non-resonant transitions are included in $\mathcal{H}^{exc}$ and $\mathcal{K}$, namely, we go beyond the Tamm−Dancoff approximation. We define the optical gap from the BSE or TDDFT as the energy of the lowest transition with a nonvanishing oscillator strength.

Optical excitations may cause sizable changes in the geometry of a molecule. Experimentally, adiabatic optical excitation energies are often available and sometimes differ largely from the vertical ones. Theoretically and computationally, geometry optimization in the excited state within the GW-BSE formalism is in principle possible, but it has only been performed for small molecules (CO and NH_3).[105] The authors obtain excellent agreement with experiment both for the relaxed geometry in the excited state and the transition energy. Alternatively, relaxed geometries can be obtained using TDDFT.[106] However, a simpler and computationally less demanding approach is the following: In order to estimate atomic relaxation effects, both vertical and adiabatic ΔSCF gaps are calculated by excluding and including geometry relaxation of the triplet excited state, respectively, of the neutral molecules:

$$E^{\mathrm{opt}}_{\mathrm{gap}}(\Delta\mathrm{SCF}) = E^{\mathrm{neutral}}_{\mathrm{tot}}(\mathrm{exc}) - E^{\mathrm{neutral}}_{\mathrm{tot}}(\mathrm{GS}) \quad (16)$$

where $E^{\mathrm{neutral}}_{\mathrm{tot}}(\mathrm{exc})$ and $E^{\mathrm{neutral}}_{\mathrm{tot}}(\mathrm{GS})$ are the total energies of the lowest triplet state and the singlet ground state of the neutral molecules. In principle, the singlet state is the one of interest, but accessing it with ΔSCF is not straightforward, whereas the triplet state can be accessed easily as the ground state with spin 1. We assume here that the relaxation energies are similar in the triplet and the singlet state, an approximation we validate by comparing, for a subset of the smaller molecules, relaxation energies as calculated within TDPBE0 (singlet) and ΔSCF (triplet). Because of its much smaller computational burden, the ΔSCF approach is also applicable to the nanoparticles at which we aim. Below and in the Supporting Information (Figure S-6 and Table S-IX), we compare the results of both approaches.

3. RESULTS

All calculated and available experimental data for the ionization energies, electron affinities, quasiparticle, and optical gaps are provided in the Supporting Information. We mainly focus here below on a synthetic description, namely, mean absolute errors (MAE) and mean absolute relative errors (MARE), and postpone the discussion to the section 4.

3.1. Errors Due to Pseudopotentials, Finite Basis, and Auxiliary Basis. Whereas the correlation part of the self-energy, Σ_c, is hardly influenced by core−valence interactions, the exchange part, Σ_x, is much more sensitive in this respect.[15,47] In order to assess the error associated with the use of pseudopotentials, we first evaluate exchange core−valence effects by comparing Hartree−Fock and PBE0 eigenvalues as provided by the NWChem code for different all-electron ("ae") and pseudopotential ("pp") basis sets. Further, as shown in the Supporting Information (Figures S-1 and S-2 and Table S-I), we compare for several molecules the G_0W_0@PBE0 HOMOs and LUMOs obtained at the all-electron aug-cc-pvqz and the aug-sbkjc-pp levels as defined above. Our results show that the pseudopotential error in G_0W_0@PBE0 is within about 0.1 eV (see Supporting Information Table S-I).

In the G_0W_0 calculations, accurate ionization energies can be obtained without augmentation functions, but the latter are essential to converge the electron affinities (see Supporting Information). The error arising from the auxiliary basis is found to be small (about 0.14 eV maximum, usually much smaller; see Supporting Information).

3.2. Geometries. The mean absolute error (MAE) of the bond lengths optimized with the "aug-sbkjc-pp" basis and the PBE0 functional is about 0.01 Å, which corresponds to a mean absolute relative error of 0.5% (cf. Table 2). The experimental and calculated bond lengths and bond angles of all molecules are listed in the Supporting Information.

3.3. Ionization Energies. In Figure 1, the absolute difference between calculated and experimental ionization

Table 2. Mean Absolute Error (MAE) and Mean Relative Absolute Error (MARE) of the Bond Lengths and Bond Angles

bond length (Å)		bond angle (deg)	
MAE	MARE (%)	MAE	MARE (%)
0.011	0.5	0.004	0.004

energies is drawn as a color map. The resulting mean-absolute error (MAE) and mean absolute relative error (MARE) are listed in Table 3. In the cases where the experimental values are adiabatic, the vertical calculated numbers have been corrected by the difference between the adiabatic and vertical ΔSCF energies. For those experimental values, for which it is unclear whether they are vertical or adiabatic (those without a superscript in the tables in the Supporting Information), the calculated values have not been corrected in the graph and left out of the average. The mean absolute errors (MAE) for the ionization energies are depicted in Figure 2.

The best *GW* result is obtained at the G_0W_0 level on top of PBE0 or scCOHSEX, yielding a MAE of 0.21 and 0.26 eV, respectively, close to the ΔSCF value of 0.29 eV. It should be mentioned that G_0W_0@PBE0 and ΔSCF both break down for the same system, Ag_3I_3). This points toward the spread of the current experimental data (see discussion) as the main source of disagreement for this molecule.

3.4. Electron Affinities. Figure 3 shows the same as Figure 1 for the electron affinities. The MAE of the electron affinities is listed in Table 3 and depicted in Figure 4. On average, G_0W_0@PBE0, scCOHSEX, and ΔSCF yield the best agreement with available experimental data.

Three molecules (TiF_4, WF_6, MoF_6) are problematic at almost all levels of theory. These molecules dominate the MAE, and, once again, this discrepancy can be attributed to the difficulty to compare with experimental conditions (see Discussion).

3.5. Quasiparticle Gaps. Comparison of our quasiparticle gaps with experiment is even less straightforward, since most experimental data for the IE are vertical, while those for the EA usually are adiabatic. In addition, the latter are less abundant. Therefore, the number of available experimental quasiparticle gaps is reduced as compared to the IE or EA individually (only 8 molecules are included). Nevertheless, we list the MAE of the quasiparticle gaps in Table 3 and depict them in Figure 5. The calculated vertical quasiparticle gaps, and in the case of ΔSCF, also the adiabatic ones, of all molecules are listed in the Supporting Information. The G_0W_0@PBE0 approach yields a very small MAE of 0.13 eV, actually smaller than the 0.18 eV

Table 3. MAE in Electron Volts and MARE in % of the Ionization Energies, Electron Affinities, and Quasiparticle Gaps

	IE		EA		E_g	
	MAE	MARE	MAE	MARE	MAE	MARE
PBE0	2.18	21.1	1.41	98.1	3.72	47.1
G_0W_0@PBE0	0.21	2.0	0.31	13.4	0.13	1.6
ev*GW*@PBE0	0.38	3.6	0.49	24.4	0.49	6.0
HF	0.86	8.4	1.20	64.0	1.51	18.0
G_0W_0@HF	0.52	5.1	0.52	31.2	0.31	3.7
ev*GW*@HF	0.47	4.7	0.54	31.7	0.26	3.0
evCOHSEX	1.92	18.4	0.28	12.9	1.55	19.4
G_0W_0@evCOHSEX	0.52	5.0	0.54	27.7	0.67	8.2
ev*GW*@evCOHSEX	0.36	3.5	0.54	27.2	0.51	6.3
scCOHSEX	1.47	14.2	0.18	9.5	1.17	14.6
G_0W_0@scCOHSEX	0.26	2.6	0.59	31.2	0.25	3.0
ev*GW*@scCOHSEX	0.30	2.9	0.58	30.6	0.27	3.2
ΔSCF	0.29	2.6	0.27	9.8	0.18	2.1

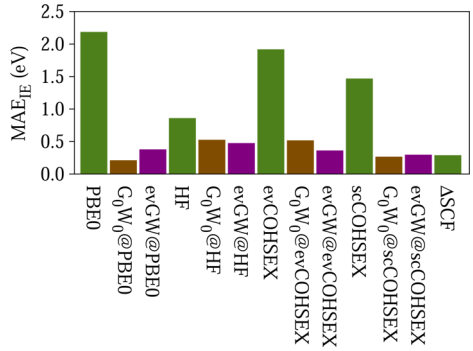

Figure 2. (Color online) MAE of the ionization energies versus theory level.

MAE of ΔSCF. This result indicates that the error within the *GW* approach can be mostly described as a rigid shift of both the HOMO and LUMO levels. This is a first indication that excitation energies should be well described within the present many-body formalism.

Besides comparison to experiment, we can compare all methods on the full set of molecules. The effect of partial self-consistency on the *GW* level, when starting from PBE0 eigenstates, is to increase the quasiparticle gaps (with a mean increase of about 0.6 eV). On the other hand, when starting from COHSEX eigenstates, which always overestimates the quasiparticle gap at the G_0W_0 level when compared to

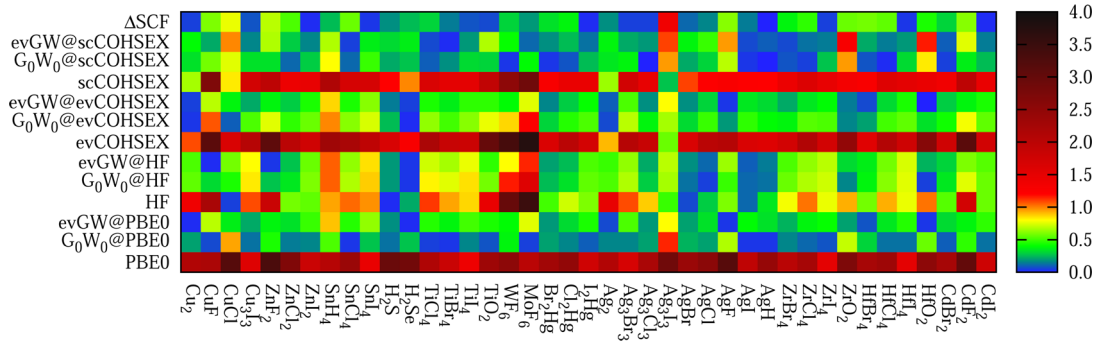

Figure 1. (Color online) Absolute difference between calculated and experimental ionization energy at different levels of theory, in electron volts.

dx.doi.org/10.1021/ct5003658 | J. Chem. Theory Comput. 2014, 10, 3934−3943

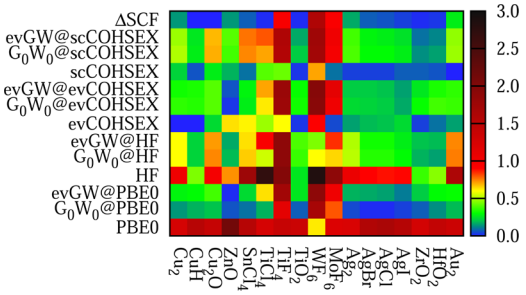

Figure 3. (Color online) Absolute difference between calculated and experimental electron affinities at different levels of theory, in electron volts.

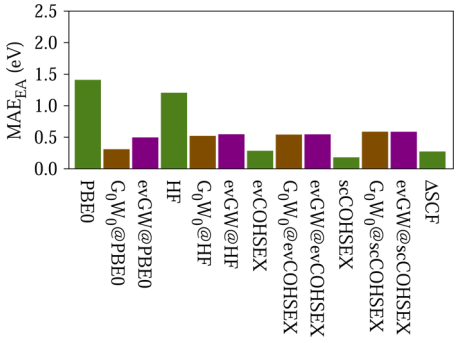

Figure 4. (Color online) MAE of the electron affinities versus theory level.

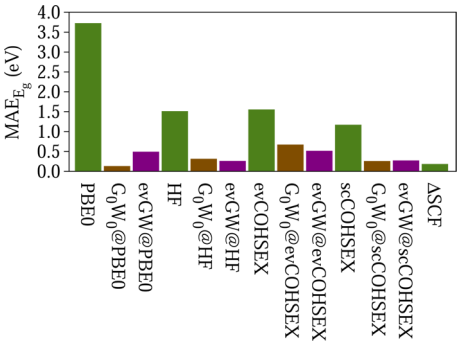

Figure 5. (Color online) MAE of the quasiparticle gaps versus theory level. Note the change of scale.

experiment, the effect of partial self-consistency is to reduce the quasiparticle gaps (with a mean decrease of 0.2 eV).

3.6. Optical Gaps. The optical gaps obtained from BSE, TDPBE0, and ΔSCF calculations are depicted in Figure 6, and their MAE are compiled in Table 4. Here, "PBE0" refers to HOMO−LUMO gaps as before, but "ΔSCF" now refers to the energy difference between the first triplet state and the singlet ground state of the neutral molecule, cf. eq 16. In Table 4, in the case of adiabatic experimental gaps, the calculated vertical energies have been corrected by the relaxation energy (Δ_r) calculated either from ΔSCF for triplets (T) or from TDPBE0 for singlets (S). In Figure 6, we plot adiabatic transitions based on the ΔSCF relaxation energies. Our BSE calculations are either started from the quasiparticle energies obtained with G_0W_0@PBE0, ev*GW*@PBE0, or scCOHSEX. For the singlet excitations, the many-body BSE@ev*GW*@PBE0 leads to an MAE of 0.3 eV, similar to the MAE of TDPBE0 (0.4 eV). For the sake of completeness, the singlet−triplet excitation energy splitting, obtained within both the BSE and TDPBE0, and the relaxation energies from ΔSCF (T) and TDPBE0 (S) are provided in the Supporting Information. Using the more appropriate, but computationally much more expensive Δ_r from TDPBE0 (S), the MAE is reduced by 0.2 eV for TDPBE0 and by 0.3 eV for BSE@G_0W_0@PBE0, respectively, bringing these theoretical data in better agreement with experiment.

4. DISCUSSION

4.1. Quasiparticle Energies. We observe that G_0W_0 calculations on top of frozen PBE0 orbitals yield the smallest MAE for the IE and the quasiparticle gaps, but since the experimental data for the IE are more numerous and probably more accurate, we will focus on this quantity in our discussion. We can note that at the G_0W_0 level, scCOHSEX is the second best starting point, with only a small (0.05 eV) increase of the MAE, which renders both methods quite similar in accuracy. On the other hand, the 0.31 eV increase of the MAE for G_0W_0@HF is a clear indication of a decreased agreement with experiment.

The effect of partial self-consistence at the ev*GW* level is to increase the MAE when starting from PBE0 eigenstates, while it has almost no effect on the MAE when scCOHSEX eigenstates are used. At this level of theory, it is ev*GW*@scCOHSEX, which gives one of the smallest MAE for all the IE and the quasiparticle gaps. This comes as no surprise, since the accuracy of the COHSEX method was shown in the case of solids containing localized *d* orbitals, where it reproduced the wave functions stemming form a fully self-consistent *GW* calculation.[107−110] The accuracy of the scCOHSEX wave functions, when compared to hybrid functionals, was also discussed for model streptocyanines,[111] where it was shown to be in better agreement with high-level coupled-cluster quantum chemistry methods. The difference of about 0.3−0.4 eV between IE from scCOHSEX and evCOHSEX calculations, respectively, provides an estimate for orbital relaxation effects in these molecules, which should be larger than in solids.[112] Another point of interest is that the ev*GW*@PBE0 and ev*GW*@evCOHSEX methods, which both use frozen PBE0 wave functions, yield the same MAE for all quantities, suggesting that the partial self-consistency effectively removes the dependence on the initial eigenenergies, leaving only the dependence on the initial wave functions.

By comparing ionization energies of a few molecules to those obtained in refs 113, 114, and 15, we estimate that our perhaps slightly different equilibrium geometries, the different basis sets, use of an auxiliary basis set, and the pseudopotentials used here, all together lead to differences of up to about 0.15 eV (see Supporting Information). For TiO_2, as a test case for small molecules containing transition metal atoms, our G_0W_0@PBE0 value for the IE (9.57 eV) at the pseudopotential level can be compared to the all-electron value of 9.46 eV, almost the same as the one of Marom and co-workers (we estimate an IE of 9.4 eV from their Figure 3).[114]

In ref 12, which considered small molecules including first and second row atoms, a MAE of 0.24 eV has been obtained for the IE stemming from ΔSCF, compared to 0.5 eV for fully self-consistent *GW* results. In the present study, the MAE for the IE is about 0.3 eV for ΔSCF, 0.2 eV for G_0W_0@PBE0 (similar to the 0.17 eV of ref 15), and 0.27 eV for ev*GW*@scCOHSEX; that is, the difference between the many-body and ΔSCF approaches is reduced for this set of molecules with transition metal atoms. However, as emphasized above, the many-body

dx.doi.org/10.1021/ct5003658 | J. Chem. Theory Comput. 2014, 10, 3934−3943

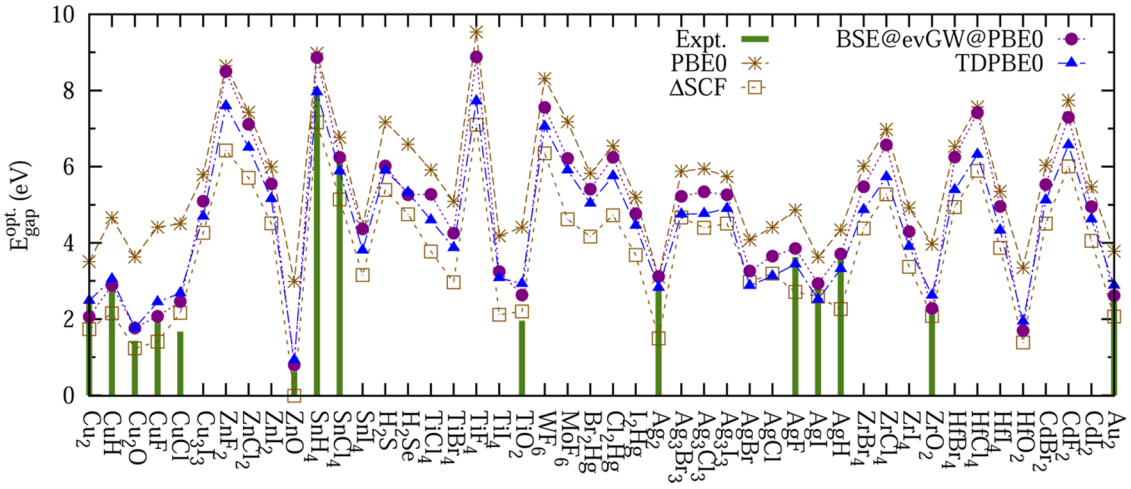

Figure 6. (Color online) Optical gaps from PBE0, ΔSCF, the BSE, and TDPBE0, compared to experimental data. The lines only serve as a guide to the eye.

Table 4. MAE (in eV) and MARE (in %) of the Optical Gaps[a]

	MAE using Δ_r (ΔSCF, T)	MARE using Δ_r (ΔSCF, T)	MAE using Δ_r (TDPBE0, S)	MARE using Δ_r (TDPBE0, S)
PBE0	1.53	73	1.95	105
BSE@G_0W_0PBE0 (S)	0.59	23	0.31	16
BSE@ev*GW*@PBE0 (S)	0.31	15	0.33	18
BSE@ev*GW*@scCOHSEX (S)	0.66	28	0.71	39
ΔSCF (T)	0.65	24		
TDPBE0 (S)	0.40	19	0.18	9

[a]With the exception of ΔSCF, all excitation energies are those of singlet excitations. In the case of adiabatic experimental excitations, the calculated vertical energies are corrected using either the triplet relaxation energies ("Δ_r (ΔSCF, T)") or the singlet relaxation energies ("Δ_r (TDPBE0, S)").

approach offers a similar accuracy as ΔSCF with the PBE0 functional while offering a parameter-free formalism which can extract all the quasiparticle spectrum.

Several points may be invoked to comment on the residual discrepancy between theory and experiment. According to ref 3 and references therein, the polarization of core electrons, neglected both in our pseudopotential- and the frozen-core approach made in ref 12, can increase ionization energies and change energy gaps by up to a few tenth of an eV in semiconductors. Further, zero-point energy contributions may, in principle, contribute to the difference between theory and experiment. However, at least in the case of the Cu_2, Ag_2, Au_2,[66,86] AgCl, AgBr, and AgI molecules,[91] differences in zero-point energies do not seem to be responsible for the observed discrepancy, because they are of the order of 0.01 eV only and go into the wrong direction.

Another important point for heavy atoms are relativistic effects, which can modify the quasiparticle states. In this paper, we use scalar relativistic pseudopotentials excluding the effect of spin−orbit coupling, which is known to close the quasiparticle gaps by up to 0.4 eV, as found for tin-based perovskites.[115] This could, in principle, partially compensate the global overestimation with respect to experiment observed in the case of ev*GW* and G_0W_0@scCOHSEX.

It should finally be emphasized that experimental values should be considered with care when discussing errors at the scale of a few tenths of an electron volt. As emphasized above, the distinction between vertical and adiabatic values is sometimes difficult to assess. In some cases, the effect of atomic relaxation in the excited state is large, for example in the case of $SnCl_4$, where it amounts to about 0.5 eV for the IE and about 0.9 eV for the EA, and needs to be taken into account to obtain satisfactory agreement between calculated and experimental electron affinity.

In general, the experimental values contain error bars of the order of up to several tenths of an electron volt. Therefore, our calculated values and their experimental counterparts can be compared only within a similar uncertainty of the order of a tenth of an electron volt. Average experimental uncertainties are about 0.1 eV for the IE, 0.2 eV for the EA, and 0.1 eV for the quasiparticle gap (see Supporting Information). For example, the ionization energy of Ag_3I_3 is systematically underestimated by about 1 eV by all theory levels applied here, with the exception of Hartree−Fock, compared to the vertical experimental value of 10.43 eV from ref 89, but it agrees much better with a different experimental value of 9.2 eV from ref 60. For CuF, the experimentally measured ionization energies scatter between 8.6 and 10.9 eV,[60] a range that includes all our many-body results.

In the case of WF_6 and MoF_6, the comparison to experiment is particularly difficult. The experimentally measured electron affinities scatter between 2.7 and 5.1 eV for WF_6 and between 3.6 and 5.8 eV for MoF_6.[60,116] Comparing to results of calculations of others, we find that our adiabatic EA of 3.30 eV for WF_6 on ev*GW*@scCOHSEX level is close to the calculated value of 3.16 eV of ref 117, obtained on CCSD(T) level, using an augmented quadruple-ζ plus polarization basis.

Finally, for TiF_4, an additional electron is only weakly bound, if no atomic relaxation is allowed, so that the vertical electron affinity is approximately zero. In this case, it is not sufficient to simply add the relaxation energy obtained from a ΔSCF calculation. However, if the electron affinity is calculated in the

dx.doi.org/10.1021/ct5003658 | J. Chem. Theory Comput. 2014, 10, 3934−3943

relaxed geometry of the TiF_4^- anion, we obtain very good agreement with experiment (on the G_0W_0@PBE0 level, EA = 2.35 eV; experiment, EA = 2.5 eV). We observe that the LUMO is visibly deformed at the geometry of the neutral molecule, compared to that of the relaxed geometry of the TiF_4^- anion. A similar strong dependence of weakly bound or unbound orbitals on the positions of the nuclei may also occur in other molecules.

4.2. Optical Gaps. The optical gaps obtained with BSE@ev*GW* on top of PBE0 (MAE ≈ 0.3 eV) and with TDPBE0 (MAE ≈ 0.2 eV) for our set of small molecules are both in reasonable agreement with experiment. The MAE of the BSE results is therefore not very different from that found by other groups for organic molecules (MAE ≈ 0.4 eV[40]) and SiH_4 (0.4 eV[24] and 0.6 eV[36]). Similarly, it was found that the TDPBE0 leads to a MAE of 0.25 eV for organic molecules.[118] Although in practice TDDFT can be very successful for optical gaps both in molecules and solids, the accuracy of the TDDFT gaps is very sensitive to the exchange-correlation functional used.[118] Whereas we expect the BSE to be transferable and predictive, in general, it is not obvious a priori for a given system how closely TDDFT gaps, obtained with a conventional functional, will resemble experimental ones. For example, TDLDA or TDPBE charge transfer excitations are located at much too low an energy, while on the contrary cyanine-like excitations are too large, two well-known failures that are cured within the BSE approach.[39,40,42,44,111]

ΔSCF calculations, computationaly very efficient, yield optical gaps that are too small on average (MAE = 0.6 eV) but are an improvement compared to the HOMO−LUMO gaps from PBE0 (MAE ≈ 1.5 eV). It should be kept in mind, however, that the ΔSCF calculations have been performed for excited triplet states, so that they are not directly comparable to the optically excited singlet states of interest here. Further, higher excited states and oscillator strengths are in general difficult to access within ΔSCF. A case, where our ΔSCF approach completely fails, is the ZnO molecule, where the first triplet state is wrongly positioned 0.28 eV (0.013 eV for the vertical excitation) below the singlet ground state by our ΔSCF calculation with the PBE0 functional. Similarly, in ref 119, it was found to lie 0.08 eV below the ground state using the B3LYP functional and an augmented quadruple-ζ-plus-polarization basis, whereas according to experiment and coupled-cluster calculations, it lies 0.25 or 0.26 eV above the singlet ground state.[119] Nevertheless, ΔSCF can yield optical gaps comparable to those of BSE calculations.[40]

Despite the fact that the quasiparticle gaps seem better described by G_0W_0@PBE0, the best optical gaps are obtained when using ev*GW*@PBE0 quasiparticle states. In fact, the BSE@G_0W_0@PBE0 excitation energies are generally underestimated with respect to the experimental optical gaps, which leads to a complete closure of the optical gap for the ZnO molecule. A closer inspection of this case shows that much of the error stems from the unrenormalized quasiparticle gap, which ev*GW* increases by ca. 0.9 eV compared to G_0W_0, whereas the exciton binding energy changes by ca. 0.2 eV. In our test set, this is generally true and explains why the bigger quasiparticle gaps of the ev*GW*@PBE0 lead to better agreement between the optical gaps obtained with the BSE and experiment.

5. SUMMARY

We have calculated ionization energies (IE), electron affinities (EA), and optical gaps for a set of small transition-metal molecules with different levels of theory. We find that G_0W_0 on top of PBE0 states yields ionization energies and electronic affinities in good agreement with available experimental values and ΔSCF calculations with the hybrid PBE0 functional. Namely, the MAE as compared to experiment is found to be 0.3 and 0.2 eV within ΔSCF and G_0W_0@PBE0, respectively, for the IE, while both techniques yield a MAE of 0.3 eV for the EA. The agreement with experiment is increased in the case of the quasiparticle gaps, for which G_0W_0@PBE0 yields an MAE of 0.1 eV. Further, optical gaps obtained from the Bethe−Salpeter equation are in reasonable agreement with experiment (MAE ≈ 0.3 eV at the BSE@ev*GW*@PBE0 and BSE@G_0W_0@PBE0 levels), offering a similar accuracy on average as TDPBE0 (MAE ≈ 0.2 eV).

While ΔSCF calculations certainly offer the best compromise for calculating the HOMO and LUMO energy levels, the self-consistent *GW* approach allows to calculate all addition and removal energies, with a N^4 scaling within the present resolution of the identity technique. Once the *GW* calculation is performed, the Bethe−Salpeter formalism offers the same computational performance as TDDFT within the standard Casida's approach, with the advantages of being suitable for a wide range of systems and yielding similar accuracy for Frenkel, Wannier, or charge-transfer excitations in finite size or extended systems. For the sake of illustration, such *GW*−BSE calculations have been performed on systems containing more than a hundred atoms.[120] The present study opens the way to studying the quasiparticle and optical properties of larger clusters containing transition metal atoms, including in particular the quaternary CZTS and CIGS systems of increasing interest in photovoltaics applications.

■ ASSOCIATED CONTENT

Ⓢ Supporting Information

Calculated and experimental geometries, ionization energies, electron affinities, and quasiparticle and optical gaps of the individual molecules, as well as the results of basis set convergence tests. This material is available free of charge via the Internet at http://pubs.acs.org.

■ AUTHOR INFORMATION

Corresponding Author

*Email: silvana.botti@polytechnique.edu.

Notes

The authors declare no competing financial interest.

■ ACKNOWLEDGMENTS

Financial support provided by the French ANR (project PANELS NR-12-BS04-0001-02) is gratefully acknowledged. X.B. and P.B. acknowledge computer time provided by the National GENCI-IDRIS Supercomputing Centers at Orsay under Contract No 2012096655 and a PRACE European Project under Contract No. 2012071258. S.K. thanks Dr. Tristan Albaret for stimulating discussions.

■ REFERENCES

(1) Szabo, A.; Ostlund, N. S. *Modern Quantum Chemistry*; Dover Publications Inc.: Mineola, NY, 1996.

(2) Onida, G.; Reining, L.; Rubio, A. *Rev. Mod. Phys.* **2002**, *74*, 601.

(3) Aryasetiawan, F.; Gunnarsson, O. *Rep. Prog. Phys.* **1998**, *61*, 237.
(4) Perdew, J. P.; Wang, Y. *Phys. Rev. B* **1992**, *45*, 13244−13249.
(5) Perdew, J. P.; Burke, K.; Ernzerhof, M. *Phys. Rev. Lett.* **1996**, *77*, 3865−3868.
(6) Becke, A. D. *J. Chem. Phys.* **1993**, *98*, 1372−1377.
(7) Adamo, C.; Barone, V. *J. Chem. Phys.* **1999**, *110*, 6158.
(8) Heyd, J.; Scuseria, G. E.; Ernzerhof, M. *J. Chem. Phys.* **2003**, *118*, 8207−8215.
(9) Muscat, J.; Wander, A.; Harrison, N. *Chem. Phys. Lett.* **2001**, *342*, 397−401.
(10) Heyd, J.; Scuseria, G. E. *J. Chem. Phys.* **2004**, *121*, 1187.
(11) Marques, M. A. L.; Vidal, J.; Oliveira, M. J. T.; Reining, L.; Botti, S. *Phys. Rev. B* **2011**, *83*, 035119.
(12) Rostgaard, C.; Jacobsen, K. W.; Thygesen, K. S. *Phys. Rev. B* **2010**, *81*, 085103.
(13) Jones, R. O.; Gunnarsson, O. *Rev. Mod. Phys.* **1989**, *61*, 689.
(14) Hedin, L. *Opt. Mater.* **1965**, *139*, A796.
(15) Bruneval, F.; Marques, M. A. L. *J. Chem. Theory Comput.* **2013**, *9*, 324−329.
(16) Bruneval, F. *Phys. Rev. Lett.* **2009**, *103*, 176403.
(17) Blase, X.; Attaccalite, C.; Olevano, V. *Phys. Rev. B* **2011**, *83*, 115103.
(18) Ke, S.-H. *Phys. Rev. B* **2011**, *84*, 205415.
(19) Foerster, D.; Koval, P.; Sánchez-Portal, D. *J. Chem. Phys.* **2011**, *135*, 074105.
(20) Körzdörfer, T.; Marom, N. *Phys. Rev. B* **2012**, *86*, 041110.
(21) Caruso, F.; Rinke, P.; Ren, X.; Scheffler, M.; Rubio, A. *Phys. Rev. B* **2012**, *86*, 081102.
(22) Bruneval, F. *J. Chem. Phys.* **2012**, *136*, 194107.
(23) Pham, T. A.; Nguyen, H.-V.; Rocca, D.; Galli, G. *Phys. Rev. B* **2013**, *87*, 155148.
(24) Grossman, J. C.; Rohlfing, M.; Mitas, L.; Louie, S. G.; Cohen, M. L. *Phys. Rev. Lett.* **2001**, *86*, 472−475.
(25) Umari, P.; Stenuit, G.; Baroni, S. *Phys. Rev. B* **2010**, *81*, 115104.
(26) Ma, Y.; Rohlfing, M.; Molteni, C. *Phys. Rev. B* **2009**, *80*, 241405.
(27) Atalla, V.; Yoon, M.; Caruso, F.; Rinke, P.; Scheffler, M. *Phys. Rev. B* **2013**, *88*, 165122.
(28) Faber, C.; Attaccalite, C.; Olevano, V.; Runge, E.; Blase, X. *Phys. Rev. B* **2011**, *83*, 115123.
(29) Rohlfing, M.; Louie, S. G. *Phys. Rev. Lett.* **1998**, *80*, 3320−3323.
(30) Vasiliev, I.; Öğüt, S.; Chelikowsky, J. R. *Phys. Rev. B* **2002**, *65*, 115416.
(31) Khare, A.; Wills, A. W.; Ammerman, L. M.; Norris, D. J.; Aydil, E. S. *Chem. Commun.* **2011**, *47*, 11721−11723.
(32) Paier, J.; Asahi, R.; Nagoya, A.; Kresse, G. *Phys. Rev. B* **2009**, *79*, 115126.
(33) Persson, C. *J. Appl. Phys.* **2010**, *107*, 053710.
(34) Botti, S.; Kammerlander, D.; Marques, M. A. *Appl. Phys. Lett.* **2011**, *98*, 241915.
(35) Rohlfing, M.; Louie, S. G. *Phys. Rev. B* **2000**, *62*, 4927.
(36) Tiago, M. L.; Chelikowsky, J. R. *Phys. Rev. B* **2006**, *73*, 205334.
(37) Palummo, M.; Hogan, C.; Sottile, F.; Bagalá, P.; Rubio, A. *J. Chem. Phys.* **2009**, *131*, 084102.
(38) Ma, Y.; Rohlfing, M.; Molteni, C. *J. Chem. Theory Comput.* **2009**, *6*, 257−265.
(39) Rocca, D.; Lu, D.; Galli, G. *J. Chem. Phys.* **2010**, *133*, 164109.
(40) Garcia-Lastra, J. M.; Thygesen, K. S. *Phys. Rev. Lett.* **2011**, *106*, 187402.
(41) Conte, A. M.; Guidoni, L.; Del Sole, R.; Pulci, O. *Chem. Phys. Lett.* **2011**, *515*, 290−295.
(42) Blase, X.; Attaccalite, C. *Appl. Phys. Lett.* **2011**, *99*, 171909−171909.
(43) Duchemin, I.; Deutsch, T.; Blase, X. *Phys. Rev. Lett.* **2012**, *109*, 167801.
(44) Baumeier, B.; Andrienko, D.; Rohlfing, M. *J. Chem. Theory Comput.* **2012**, *8*, 2790−2795.
(45) Valiev, M.; Bylaska, E. J.; Govind, N.; Kowalski, K.; Straatsma, T. P.; Van Dam, H. J.; Wang, D.; Nieplocha, J.; Apra, E.; Windus, T. L.; de Jong, W. A. *Comput. Phys. Commun.* **2010**, *181*, 1477−1489.
(46) Hybertsen, M. S.; Louie, S. G. *Phys. Rev. B* **1986**, *34*, 5390−5413.
(47) Bruneval, F. Ph.D. Thesis, Ecole Polytechnique, Palaiseau, 2005.
(48) Ku, W.; Eguiluz, A. G. *Phys. Rev. Lett.* **2002**, *89*, 126401.
(49) Tiago, M. L.; Ismail-Beigi, S.; Louie, S. G. *Phys. Rev. B* **2004**, *69*, 125212.
(50) Delaney, K.; García-González, P.; Rubio, A.; Rinke, P.; Godby, R. W. *Phys. Rev. Lett.* **2004**, *93*, 249701.
(51) Binkley, J. S.; Pople, J. A.; Hehre, W. J. *J. Am. Chem. Soc.* **1980**, *102*, 939−947.
(52) Stevens, W. J.; Basch, H.; Krauss, M. *J. Chem. Phys.* **1984**, *81*, 6026.
(53) Stevens, W. J.; Krauss, M.; Basch, H.; Jasien, P. G. *Can. J. Chem.* **1992**, *70*, 612−630.
(54) Peterson, K. A. *J. Chem. Phys.* **2003**, *119*, 11099.
(55) Peterson, K. A.; Figgen, D.; Goll, E.; Stoll, H.; Dolg, M. *J. Chem. Phys.* **2003**, *119*, 11113.
(56) Peterson, K. A.; Puzzarini, C. *Theor. Chem. Acc.* **2005**, *114*, 283−296.
(57) Rohlfing, M.; Krüger, P.; Pollmann, J. *Phys. Rev. B* **1995**, *52*, 1905.
(58) Feyereisen, M.; Fitzgerald, G.; Komornicki, A. *Chem. Phys. Lett.* **1993**, *208*, 359−363.
(59) Skylaris, C.-K.; Gagliardi, L.; Handy, N. C.; Ioannou, A. G.; Spencer, S.; Willetts, A. *J. Mol. Struct.: THEOCHEM* **2000**, *501*, 229−239.
(60) National Institute of Standards and Technology (NIST), *Chemistry WebBook*, http://webbook.nist.gov/chemistry/ (accessed 2013).
(61) *CRC Handbook of Chemistry and Physics*, 91st ed.; Haynes, W. M., Ed.; Taylor & Francis: Boca Raton, FL, 2010.
(62) Wang, L.-S.; Wu, H.; Desai, S. R.; Lou, L. *Phys. Rev. B* **1996**, *53*, 8028.
(63) Lee, E. P.; Potts, A. W. *Chem. Phys. Lett.* **1980**, *76*, 532−536.
(64) Woods, L. *Opt. Mater.* **1943**, *64*, 259.
(65) Rao, P. M. R.; Rao, P. R. *Spectrosc. Lett.* **1974**, *7*, 463−468.
(66) Sappey, A. D.; Harrington, J. E.; Weisshaar, J. C. *J. Chem. Phys.* **1989**, *91*, 3854.
(67) Leopold, D. G.; Ho, J.; Lineberger, W. C. *J. Chem. Phys.* **1987**, *86*, 1715−1726.
(68) Calvi, R.; Andrews, D. H.; Lineberger, W. C. *Chem. Phys. Lett.* **2007**, *442*, 12−16.
(69) Potts, A. W.; Lyus, M. L. *J. Electron Spectrosc. Relat. Phenom.* **1978**, *13*, 305−315.
(70) Dyke, J. M.; Fayad, N. K.; Josland, G. D.; Morris, A. *J. Chem. Soc., Faraday Trans. 2* **1980**, *76*, 1672−1682.
(71) Wang, L.-S.; Niu, B.; Lee, Y.; Shirley, D. *J. Chem. Phys.* **1990**, *93*, 957−966.
(72) Cocksey, B. G.; Eland, J. H. D.; Danby, C. J. *J. Chem. Soc., Faraday Trans. 2* **1973**, *69*, 1558−1561.
(73) Fancher, C.; De Clercq, H.; Thomas, O.; Robinson, D.; Bowen, K. *J. Chem. Phys.* **1998**, *109*, 8426.
(74) Moravec, V. D.; Klopcic, S. A.; Chatterjee, B.; Jarrold, C. C. *Chem. Phys. Lett.* **2001**, *341*, 313−318.
(75) Potts, A. W.; Price, W. 1972, *326*, 165−179.
(76) Fernandez, J.; Lespes, G.; Dargelos, A. *Chem. Phys.* **1986**, *103*, 85−91.
(77) Bassett, P.; Lloyd, D. *J. Chem. Soc. A* **1971**, 641−645.
(78) Mathur, B.; Rothe, E. W.; Reck, G. P. *Int. J. Mass Spectrom. Ion Phys.* **1979**, *31*, 77−84.
(79) Lacmann, K.; Maneira, M.; Moutinho, A.; Weigmann, U. *J. Chem. Phys.* **1983**, *78*, 1767−1776.
(80) Causley, G.; Russell, B. *J. Electron Spectrosc. Relat. Phenom.* **1977**, *11*, 383−397.
(81) Burroughs, P.; Evans, S.; Hamnett, A.; Orchard, A. F.; Richardson, N. V. *J. Chem. Soc., Faraday Trans. 2* **1974**, *70*, 1895−1911.
(82) Al-Joboury, M.; Turner, D. *J. Chem. Soc.* **1964**, 4434−4441.

(83) Delwiche, J.; Natalis, P.; Collin, J. *Int. J. Mass Spectrom. Ion Phys.* **1970**, *5*, 443−455.
(84) Beutel, V.; Krämer, H.-G.; Bhale, G.; Kuhn, M.; Weyers, K.; Demtröder, W. *J. Chem. Phys.* **1993**, *98*, 2699−2708.
(85) Handschuh, H.; Cha, C.-Y.; Bechthold, P. S.; Ganteför, G.; Eberhardt, W. *J. Chem. Phys.* **1995**, *102*, 6406−6422.
(86) Ho, J.; Ervin, K. M.; Lineberger, W. *J. Chem. Phys.* **1990**, *93*, 6987.
(87) Fedrigo, S.; Harbich, W.; Buttet, J. *Phys. Rev. B* **1993**, *47*, 10706.
(88) MacNaughton, R.; Bloor, J.; Sherrod, R.; Schweitzer, G. K. *J. Electron Spectrosc. Relat. Phenom.* **1981**, *22*, 1−25.
(89) MacNaughton, R.; Allen, J.; Schweitzer, G. *J. Electron Spectrosc. Relat. Phenom.* **1980**, *18*, 363−367.
(90) Berkowitz, J.; Batson, C.; Goodman, G. *J. Chem. Phys.* **1980**, *72*, 5829−5837.
(91) Wu, X.; Xie, H.; Qin, Z.; Tan, K.; Tang, Z.; Lu, X. *J. Phys. Chem. A* **2011**, *115*, 6321−6326.
(92) Hildenbrand, D. *J. Chem. Phys.* **1977**, *66*, 4788−4794.
(93) Chen, Y.-M.; Armentrout, P. *J. Phys. Chem.* **1995**, *99*, 11424−11431.
(94) Ames, L.; Barrow, R. *Trans. Faraday Soc.* **1967**, *63*, 39−44.
(95) Cox, P.; Evans, S.; Hamnett, A.; Orchard, A. *Chem. Phys. Lett.* **1970**, *7*, 414−416.
(96) Green, J.; Green, M.; Joachim, P. J.; Orchard, A.; Turner, D. *Philos. Trans. R. Soc., A* **1970**, *268*, 111−130.
(97) Egdell, R. G.; Orchard, A. F. *J. Chem. Soc., Faraday Trans. 2* **1978**, *74*, 485−500.
(98) Hildenbrand, D. *Chem. Phys. Lett.* **1976**, *44*, 281−284.
(99) Wu, H.; Wang, L.-S. *J. Chem. Phys.* **1997**, *107*, 8221−8228.
(100) Rauh, E.; Ackermann, R. *J. Chem. Phys.* **1974**, *60*, 1396−1400.
(101) Kim, J. B.; Weichman, M. L.; Neumark, D. M. *Phys. Chem. Chem. Phys.* **2013**, *15*, 20973−20981.
(102) Eland, J. *Int. J. Mass Spectrom. Ion Phys.* **1970**, *4*, 37−49.
(103) Bloor, J.; Sherrod, R. *J. Am. Chem. Soc.* **1980**, *102*, 4333−4340.
(104) Sottile, F. Ph.D. Thesis, Ecole Polytechnique, Palaiseau, 2003.
(105) Ismail-Beigi, S.; Louie, S. G. *Phys. Rev. Lett.* **2003**, *90*, 076401.
(106) Caillie, C. V.; Amos, R. D. *Chem. Phys. Lett.* **1999**, *308*, 249−255.
(107) Bruneval, F.; Vast, N.; Reining, L.; Izquierdo, M.; Sirotti, F.; Barrett, N. *Phys. Rev. Lett.* **2006**, *97*, 267601.
(108) Bruneval, F.; Vast, N.; Reining, L. *Phys. Rev. B* **2006**, *74*, 045102.
(109) Gatti, M.; Bruneval, F.; Olevano, V.; Reining, L. *Phys. Rev. Lett.* **2007**, *99*, 266402.
(110) Vidal, J.; Botti, S.; Olsson, P.; Guillemoles, J.-F.; Reining, L. *Phys. Rev. Lett.* **2010**, *104*, 056401.
(111) Boulanger, P.; Jacquemin, D.; Duchemin, I.; Blase, X. *J. Chem. Theory Comput.* **2014**, *10*, 1212−1218.
(112) Kaasbjerg, K.; Thygesen, K. S. *Phys. Rev. B* **2010**, *81*, 085102.
(113) Ren, X.; Rinke, P.; Blum, V.; Wieferink, J.; Tkatchenko, A.; Sanfilippo, A.; Reuter, K.; Scheffler, M. *New J. Phys.* **2012**, *14*, 053020.
(114) Marom, N.; Moussa, J. E.; Ren, X.; Tkatchenko, A.; Chelikowsky, J. R. *Phys. Rev. B* **2011**, *84*, 245115.
(115) Umari, P.; Mosconi, E.; De Angelis, F. *Sci. Rep.* **2014**, *4*, 4467.
(116) Sidorov, L.; Borshchevsky, A. Y.; Rudny, E.; Butsky, V. *Chem. Phys.* **1982**, *71*, 145−156.
(117) Craciun, R.; Picone, D.; Long, R. T.; Li, S.; Dixon, D. A.; Peterson, K. A.; Christe, K. O. *Inorg. Chem.* **2010**, *49*, 1056−1070.
(118) Jacquemin, D.; Wathelet, V.; Perpète, E. A.; Adamo, C. *J. Chem. Theory Comput.* **2009**, *5*, 2420−2435.
(119) Bauschlicher, C. W., Jr; Partridge, H. *J. Chem. Phys.* **1998**, *109*, 8430.
(120) Duchemin, I.; Blase, X. *Phys. Rev. B* **2013**, *87*, 245412.